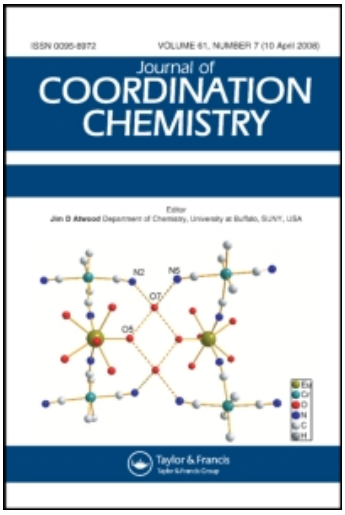

Journal of Coordination Chemistry
Publication details, including instructions for authors and subscription information:
http://www.informaworld.com/smpp/title~content=t713455674

Two pillared-layer architectures constructed from copper molybdate sheets and linear organonitrogen ligands

Yuhua Feng[a]; Jun Peng[b]; Xiquan Che[a]; Yuxiang Gao[a]
[a] Department of Chemistry, Tonghua Teachers College, Tonghua, People's Republic of China [b] Faculty of Chemistry, Institute of Polyoxometalate Chemistry, Northeast Normal University, Changchun, People's Republic of China

To cite this Article Feng, Yuhua , Peng, Jun , Che, Xiquan and Gao, Yuxiang(2006) 'Two pillared-layer architectures constructed from copper molybdate sheets and linear organonitrogen ligands', Journal of Coordination Chemistry, 59: 12, 1349 — 1359
To link to this Article: DOI: 10.1080/00958970500537549
URL: http://dx.doi.org/10.1080/00958970500537549

Journal of Coordination Chemistry
Vol. 59, No. 12, 5 August 2006, 1349–1359

Taylor & Francis
Taylor & Francis Group

Two pillared-layer architectures constructed from copper molybdate sheets and linear organonitrogen ligands

YUHUA FENG*†, JUN PENG*‡, XIQUAN CHE† and YUXIANG GAO†

†Department of Chemistry, Tonghua Teachers College, Tonghua, 134002, People's Republic of China
‡Faculty of Chemistry, Institute of Polyoxometalate Chemistry, Northeast Normal University, Changchun, 130024, People's Republic of China

(*Received 7 August 2005*)

In this article, we report the syntheses and structures of two new inorganic–organic hybrid copper molybdates with organonitrogen ligands, $[Cu_2(bpe)(Mo_2O_8)]\cdot 3H_2O$ (**1**) (bpe = 1,2-bis(4-pyridyl)ethene) and $[\{Cu(4,4'\text{-bpy})\}_2(Mo_2O_8)]$ (**2**) (bpy = 4,4′-bipyridine). Elemental analyses, IR spectra, EPR spectra, XPS spectra, TG analyses and single crystal X-ray diffraction were used to characterize these compounds. The structure of **1** exhibits a pillared-layer framework built up from unusual bimetallic two-dimensional sheets pillared by linear bpe ligands. Compound **2** features a pillared-layer structure constructed from copper molybdate 4,8-net sheets connected by 4,4′-bpy ligands.

Keywords: Pillared-layer; Inorganic–organic; Hybrid; Crystal structure

1. Introduction

Organic–inorganic hybrid solids have captured considerable attention because of their distinctive topological structures and versatile applications in fields, such as catalysis and materials science [1–4]. Integration of metal-organic complexes and molybdenum oxide moieties into a single structure is a subclass of organic–inorganic hybrid materials [5–8], which exhibit diversified multi-dimensional structures. Recently, the rational design of organic–inorganic molybdenum oxide phases was achieved in defining their structures with control of the synergistic interaction between organic and inorganic fragments, providing a route to the goal because there is a correlation between the structure of a material and its functionality [9, 10]. Some hybrid metal molybdate complexes are reported with fascinating architectures including helical and chiral structures [11]. Pillared-layer structures, which have proven to be an effective and controllable route to 3-D frameworks with large channels, received attention

*Corresponding authors. Email: fengyh009@126.com; jpeng@nenu.edu.cn

Journal of Coordination Chemistry
ISSN 0095-8972 print: ISSN 1029-0389 online © 2006 Taylor & Francis
DOI: 10.1080/00958970500537549

because of their distinct structural feature of changeable pillaring fragments in the interlamellar regions [11–16]. Typically, hybrid solids and coordination polymers with pillared-layer structures can be obtained by exploiting linear organic ligands or functional groups to connect two-dimensional inorganic moieties or polymer subunits [17]. Extension of layered molybdate moieties into pillared-layer structures is reasonable by connection of linear organic ligands and secondary metal (mainly transition metal) sites embedded in the molybdate structures.

In this work, we report the syntheses and structures of two pillared-layer compounds isolated by introduction of linear organonitrogen ligands into the copper molybdate systems, $\{Cu_2(bpe)(Mo_2O_8)\} \cdot 3H_2O$ (**1**) (bpe = 1,2-bis(4-pyridyl)ethene) and $[\{Cu(4,4'\text{-bpy})\}_2(Mo_2O_8)]$ (**2**) (bpy = 4,4′-bipyridine). The structure of **1** exhibits a pillared-layer framework built up from unusual bimetallic two-dimensional sheets pillared by linear bpe ligands. Compound **2** features a pillared-layer structure constructed from copper molybdate 4,8-net sheets connected by 4,4′-bpy ligands.

2. Results and discussion

2.1. *Description of the structures*

2.1.1. Structure of compound 1. Single crystal X-ray diffraction analysis reveals that the structure of compound **1** consists of $\{MoO_4\}$ tetrahedra, $\{CuO_5N\}$ octahedra and bpe molecules. The basic building block of **1** is shown in figure 1. The two crystallographically independent Mo sites are occupied by a $\{Mo(1)O_4\}$ tetrahedra and $\{Mo(2)O_4\}$ tetrahedra. There are two crystallographically independent Cu atoms in the asymmetric unit: the Cu(3) atom, residing in a distorted octahedral environment, is coordinated by one nitrogen atom from a bpe ligand with a Cu–N distance of 1.981 Å, and five bridging oxygen atoms with Cu–O bond lengths from 1.951 to 2.373 Å, two of which are linked with Mo(1) atom and the other three linked with Mo(2); the Cu(4) binds to one nitrogen atom and four oxygen atoms from $\{Mo(1)O_4\}$ or $\{Mo(1)O_4\}$ tetrahedra with the Cu–N distance of 2.003 Å and the Cu–O bond lengths vary from 1.926 to 2.453 Å, with a little longer Cu(4)–O(6), indicating that the Cu(4) site is an elongate octahedral environment.

The bimetallic sheet in **1** contains two types of copper molybdate ribbons constructed from alternative $\{CuNO_5\}$ and $\{MoO_4\}$ polyhedra in corner- or edge-sharing modes (figure 3). Interestingly, these two types of ribbons are further connected to each other by sharing bridging $\{CuNO_5\}$ or $\{MoO_4\}$ oxygen atoms to form a pleat layer with dihedral angles of about 53°. The extension of the structure is realized by means of the covalent bridging of bpe ligands to Cu(3) and Cu(4) sites which result in a pillared coordination framework with channels running along *a* and *b* axes (see figure 4). Three crystallographically independent water molecules fill in the void of the pillaring regions.

2.1.2. Structure of compound 2. The crystal structure of **2** is assembled from a copper molybdate 4,8-net sheet covalently attached via pillaring 4,4′-bpy ligands. The two crystallographically independent Mo sites are occupied by $\{MoO_4\}$ tetrahedra. The two crystallographically unique Cu atoms both coordinate to two nitrogen atoms

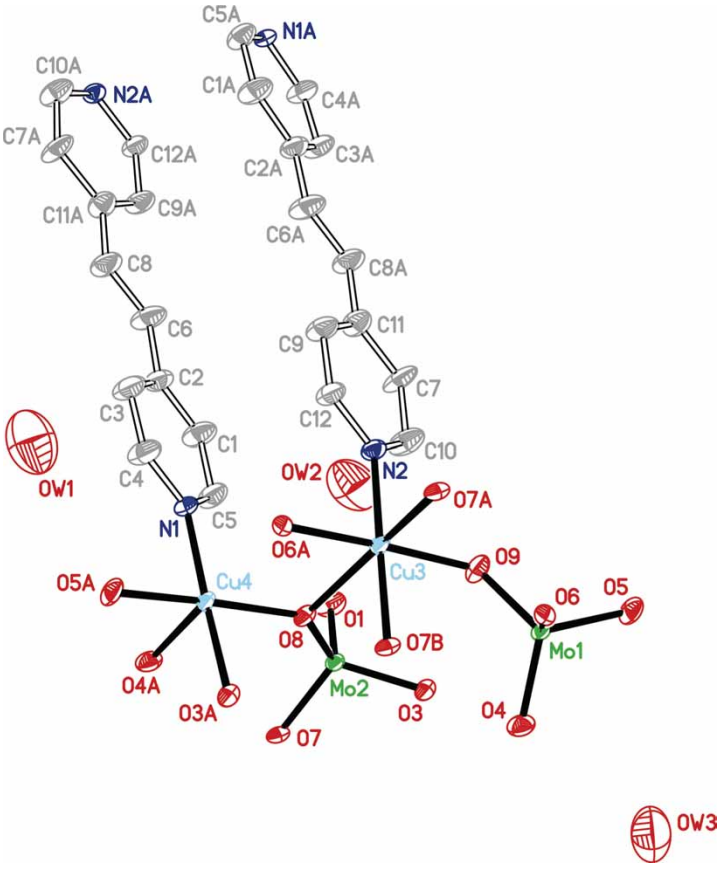

Figure 1. ORTEP drawing of **1** showing the coordination environment around Cu and Mo with thermal ellipsoids at 50% probability. For the sake of clarity, all hydrogen atoms are omitted.

from two bpe ligands, and three oxygen atoms (see figure 2). The Cu–N distances vary from 2.002 to 2.029 Å and the Cu–O bond lengths range from 1.951 to 2.115 Å. The N–Cu–O angles are in the range of 87.89–92.01° and 87.46–92.08° for the two Cu atoms respectively, indicating that the two sites reside in a trigonal bipyramidal environment.

The pillared-layer scaffolding of **2** can be divided into two parts, the layered copper molybdate subunits and the pillaring 4,4′-bpy ligands. The $\{CuN_2O_3\}$ and $\{MoO_4\}$ polyhedra link to each other in a corner-sharing fashion to construct a uniform 4,8-net sheet (figure 5), in which eight-membered $\{Cu_2Mo_2O_4\}$ and the sixteen-membered $\{Cu_4Mo_4O_8\}$ rings are observed. The linear 4,4′-bpy ligands coordinate to the copper sites from the opposite position to form a pillared-layer structure (see figure 6).

2.2. *Discussions*

In contrast to the previously reported pillared-layer structure of $[Cu(bpe)MoO_4]$, a hybrid copper molybdate containing bpe ligands [10], the individual layers in these two compounds are different. The layer in $[Cu(bpe)MoO_4]$ is a uniform sheet

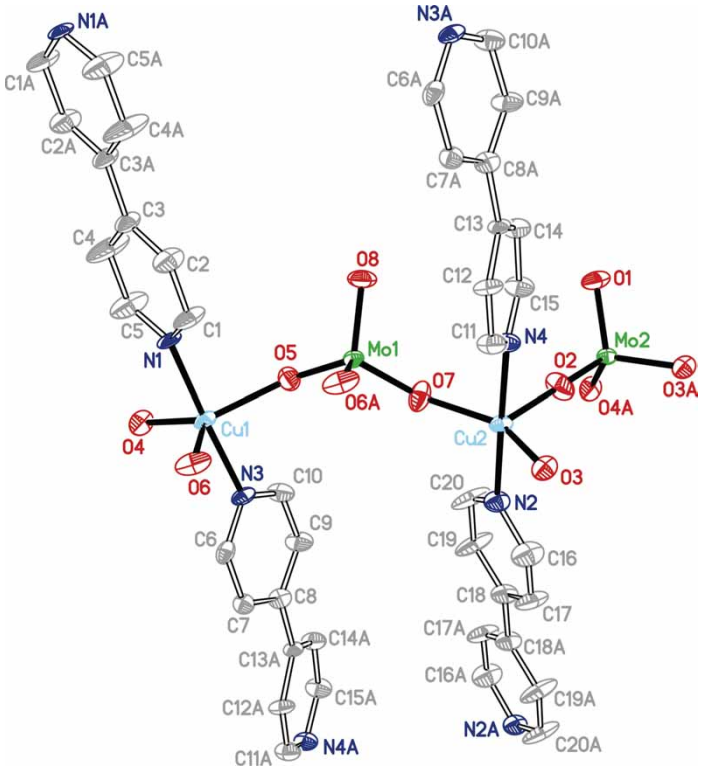

Figure 2. ORTEP drawing of the basic building block of **2** showing the coordination environment around Cu and Mo with thermal ellipsoids at 50% probability. Hydrogen atoms are omitted for clarity.

constructed by twelve-membered $\{Cu_3Mo_3O_6\}$ rings, while **1** possesses an unusual pleat sheet built from the interconnection of two types of 1-D ribbons. Another pillared-layer copper molybdate constructed by 4,4′-bpy, $[Cu_2Mo_2O_8(4,4'\text{-bpy})]_n \cdot 3nH_2O$, has a 2-D layer containing helical chains [11], different from the 4,8-net sheet observed in **2** although the same organic ligands were introduced. It is probably because of the different coordination styles of the nitrogen donors in formation of different metal-organic fragments, Cu(bpe) (for **1**), $Cu(bpe)_2$ (for $[Cu(bpe)MoO_4]$), $Cu(4,4'\text{-bpy})_2$ (for **2**), and Cu(4,4′-bpy) (for $[Cu_2Mo_2O_8(4,4'\text{-bpy})]_n \cdot 3nH_2O$), illustrating the function of metal-organic fragments for "tailoring" the microstructure of inorganic solid phases. Linear organonitrogen ligands are very useful in constructing pillared-layer structures by rational design.

3. Characterizations

3.1. *X-ray photoelectron spectra (XPS)*

The X-ray photoelectron spectra (XPS) measurements of compounds **1** and **2** in the energy region of $Mo3d_{3/2}$ and $Mo3d_{5/2}$ give two peaks (the higher at 231.9 and 232.0 eV, respectively), attributed to Mo^{6+} [18] (see figure S1). The results are in accord with the valence sum calculations for Mo^{6+} and also confirm the structure analysis.

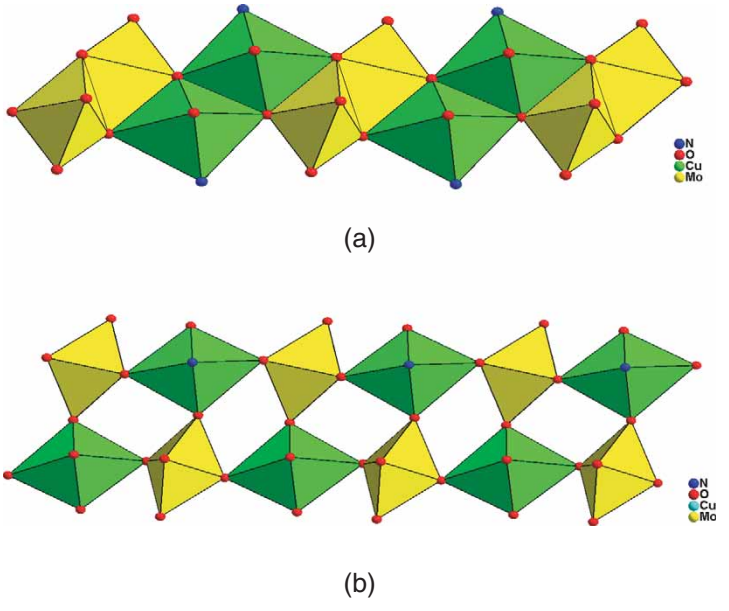

Figure 3. Polyhedral representation of the two types of bimetallic chains in the 2-D layers of compound **1**.

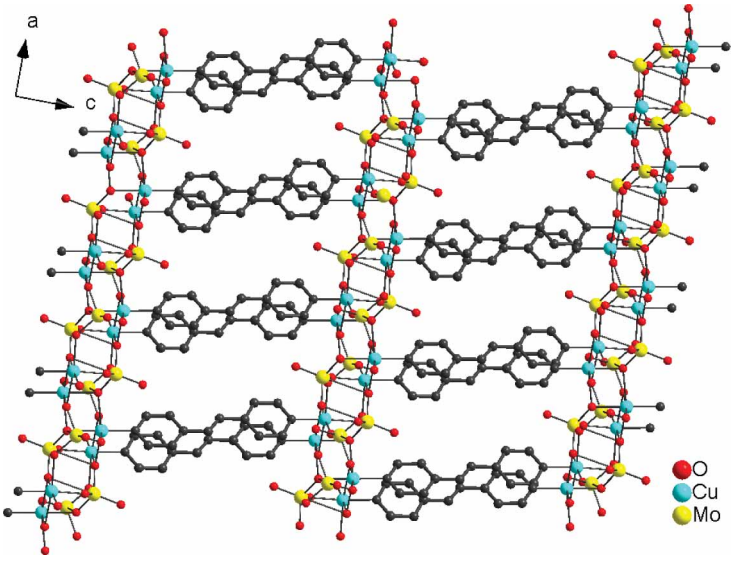

Figure 4. Ball-and-stick representation of the 3-D pillared-layer framework of compound **1**. For the sake of clarity, all the hydrogen atoms and tumbling water molecules are omitted.

3.2. EPR spectra

The EPR spectrum of **1** at room temperature shows a Cu^{2+} signal with $g = 2.065$, $g_\beta = 2.164$ (see figure S2a), in accord with the valence sum calculations for the copper

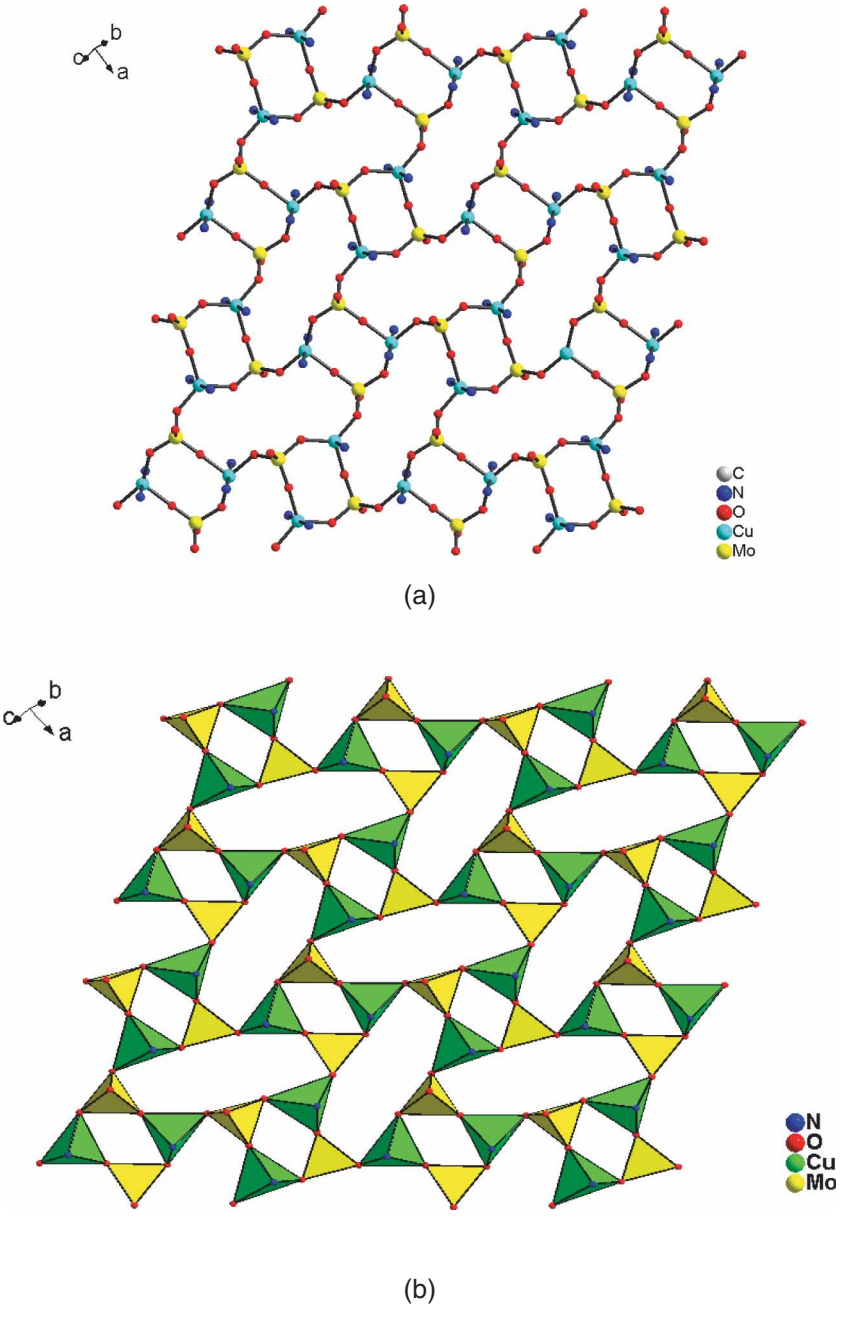

Figure 5. A view of the (a) ball-and-stick and (b) polyhedral representation of the 2-D 4,8 net in **2**.

centers in **1**. The EPR spectrum of **2** at room temperature shows a Cu^{2+} signal with $g = 2.094$, $g_\beta = 2.379$ (see figure S2b) [19]. These results further confirm the structures of **1** and **2**. The paramagnetic Cu(II) centers in compounds **1** and **2** may endow these copper molybdates with potential magnetic properties.

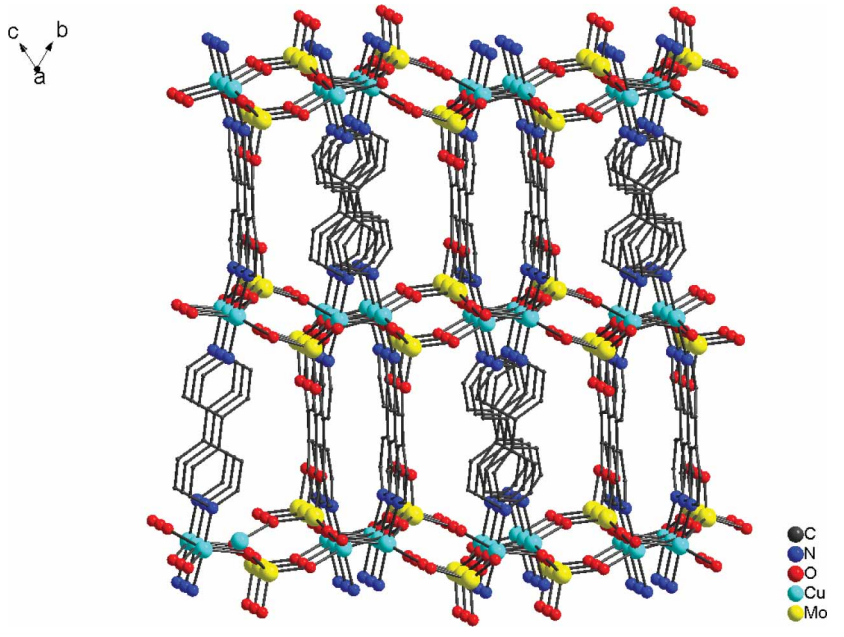

Figure 6. A view of the 3-D pillared-layer framework of **2**. For the sake of clarity, all the hydrogen atoms are omitted.

3.3. *TG analyses*

The TG curve of compound **1** exhibits two weight losses, as shown in figure S3a. The first weight loss is 7.38% from 80 to 130°C, assigned to the loss of uncoordinated water molecules (calculated value 7.93%). The compound is stable to 380°C with the second weight loss of 26.66% from 380 to 580°C, attributable to the loss of bpe ligands (calculated value 26.46%). The whole weight loss is 34.04%, in good agreement with a calculated value 34.39% (calculated as the residual composition is the mixture of CuO and MoO_3).

The TG curve of compound **2** reveals a one-step continuous weight loss (see figure S3b) in the range 350–500°C of 40.63%, corresponding to decomposition of the organic ligands. The result is in good agreement with the calculated value 41.13% (calculated as the residual composition is a mixture of CuO and MoO_3).

4. Conclusion

In summary, two new inorganic–organic hybrid copper molybdates with organonitrogen ligands have been reported. These compounds display pillared-layer frameworks with linear organic ligands as pillars. These compounds confirm that introduction of linear organic ligands as pillars for the construction of pillared-layer hybrid phases, even open frameworks with considerable voids, is an attainable goal. Future research will focus on exploring the effects of the organic ligands on the reaction.

5. Experimental

5.1. *General procedures*

All chemicals purchased were of reagent grade and used without further purification. The hydrothermal reactions were performed in 18 mL Teflon-lined stainless steel vessels under autogenous pressure filled to approximately 60%. Distilled water is used in the reactions. Elemental analyses (C and N) were performed on a Perkin-Elmer 2400 CHN Elemental Analyzer. Mo and Cu were determined by a Leaman inductively coupled plasma (ICP) spectrometer. Infrared spectra were obtained on an Alpha Centaurt FT/IR spectrometer with KBr pellets in the 4000–400 cm^{-1} region. EPR spectra were recorded on a Brucker ER 200D spectrometer at room temperature. X-ray photoelectron spectrum (XPS) analyses were performed on a VG ESCALAB MK II spectrometer with a Mg-Kα (1253.6 eV) achromatic X-ray source. The vacuum inside the analysis chamber was maintained at 6.2×10^{-6} Pa during analysis. TG analysis was performed on a Perkin-Elmer TGA7 instrument in flowing N_2 with a heating rate of $10^{\circ}C\,min^{-1}$.

5.2. *Synthesis of 1*

Compound **1** was isolated by a typical one-pot hydrothermal reaction from the mixture of $Na_2MoO_4 \cdot 2H_2O$, $Cu(CH_3COO)_2 \cdot H_2O$, 1,2-bis(4-pyridyl)ethene, and H_2O with a molar ratio of 4 : 1 : 1 : 555 under autogenous pressure at 150°C for five days. After cooling to room temperature, the sapphire-colored blocks of **1** were collected as a monophase product (about 63% yield on Cu). Anal. Calcd for $C_{12}H_{14}Mo_2N_2Cu_2O_{11}$: C, 21.16; N, 4.11; Cu, 18.66; Mo, 28.17 (%). Found: C, 20.47; N, 4.63; Cu, 19.02; Mo, 28.41 (%). IR (KBr pellet, cm^{-1}): 1633(m), 1058(m), 925(m), 806(s), and 655(s).

5.3. *Synthesis of 2*

Compound **2** was obtained by similar reaction procedure as for **1** from a mixture of $Na_2MoO_4 \cdot 2H_2O$, $Cu(CH_3COO)_2 \cdot H_2O$, 4,4′-bipyridine, and H_2O with a molar ratio of 4 : 1 : 1 : 555 under autogenous pressure at 160°C for five days. After cooling to room temperature, dark-green crystals of **2** were collected as a monophase product (about 50% yield on Cu). Anal. Calcd for $C_{20}H_{16}Mo_2N_4Cu_2O_8$: C, 31.63; N, 7.38; Cu, 16.74; Mo, 25.27 (%). Found: C, 31.41; N, 7.93; Cu, 15.94; Mo, 25.47 (%). IR (KBr pellet, cm^{-1}): 1614(s), 984(m), 918(s), 796(s), and 628(s).

6. Structural determination

The data was collected on a Rigaku R-AXIS RAPID IP diffractometer at 293 K using graphite-monochromated Mo-Kα radiation ($\lambda = 0.71073$ Å) and the oscillation scans technique in the range of $3.13^{\circ} < \theta < 27.47^{\circ}$; empirical absorption correction was applied. A total of 9632 (3474 unique, $R_{int} = 0.0685$) reflections were measured.

Table 1. Crystal data and structure refinement for compounds **1** and **2**.

	1	**2**
Empirical formula	$C_{12}H_{14}Cu_2Mo_2N_2O_{11}$	$C_{20}H_{16}Cu_2Mo_2N_4O_8$
Formula weight	681.23	759.33
Temperature (K)	293(2)	293(2)
Wavelength (Å)	0.71073	0.71073
Crystal system	Triclinic	Triclinic
Space group	$P\bar{1}$	$P\bar{1}$
a (Å)	7.4455(2)	9.812(2)
b (Å)	9.2175(2)	11.507(2)
c (Å)	15.230(3)	11.987(2)
α (°)	79.32(3)	62.07(3)
β (°)	87.31(3)	75.54(3)
γ (°)	72.85(3)	78.01(3)
Volume (Å^3)	981.4(3)	1151.3(4)
Z	2	2
Reflections collected	9632	8093
Independent reflections	4432 ($R_{int} = 0.0515$)	5198 ($R_{int} = 0.0552$)
Goodness-of-fit on F^2	0.903	1.124
Final R indices [$I > 2\sigma(I)$]	R_1[a] = 0.0438, wR_2[b] = 0.1197	R_1[a] = 0.0482, wR_2[b] = 0.1379
Indices (all data)	R_1[a] = 0.0612, wR_2[b] = 0.1355	R_1[a] = 0.0655, wR_2[b] = 0.1549

[a] $R_1 = \Sigma||F_o| - |F_c||/\Sigma|F_o|$.
[b] $wR_2 = \{\Sigma[w(F_o^2 - F_c^2)^2]/\Sigma[w(F_o^2)^2]\}^{1/2}$.

Table 2. Selected bond lengths (Å) and angles (°) for compound **1**.[a]

Mo(1)–O(4)	1.740(4)	Mo(2)–O(1)	1.700(4)
Mo(1)–O(5)	1.747(5)	Mo(2)–O(3)	1.774(4)
Mo(1)–O(9)	1.786(4)	Mo(2)–O(7)	1.783(4)
Mo(1)–O(6)	1.791(4)	Mo(2)–O(8)	1.805(4)
Cu(3)–O(9)	1.951(5)	Cu(4)–O(5)#4	1.926(5)
Cu(3)–N(2)	1.981(5)	Cu(4)–O(3)#2	1.990(4)
Cu(3)–O(6)#1	1.985(4)	Cu(4)–N(1)	2.003(5)
Cu(3)–O(7)#2	2.026(4)	Cu(4)–O(8)	2.015(4)
Cu(3)–O(7)#3	2.364(4)	Cu(4)–O(4)#2	2.325(4)
Cu(3)–O(8)	2.373(4)		
O(4)–Mo(1)–O(5)	108.8(2)	O(1)–Mo(2)–O(3)	107.0(2)
O(4)–Mo(1)–O(9)	112.2(2)	O(1)–Mo(2)–O(7)	108.0(2)
O(5)–Mo(1)–O(9)	107.2(2)	O(3)–Mo(2)–O(7)	111.5(2)
O(4)–Mo(1)–O(6)	109.8(2)	O(1)–Mo(2)–O(8)	107.0(2)
O(5)–Mo(1)–O(6)	105.9(2)	O(3)–Mo(2)–O(8)	111.9(2)
O(9)–Mo(1)–O(6)	112.6(2)	O(7)–Mo(2)–O(8)	111.1(2)
O(9)–Cu(3)–N(2)	93.2(2)	O(5)#4–Cu(4)–O(3)#2	88.63(19)
O(9)–Cu(3)–O(6)#1	171.63(17)	O(5)#4–Cu(4)–N(1)	90.0(2)
N(2)–Cu(3)–O(6)#1	93.0(2)	O(3)#2–Cu(4)–N(1)	175.4(2)
O(9)–Cu(3)–O(7)#2	86.17(18)	O(5)#4–Cu(4)–O(8)	173.92(17)
N(2)–Cu(3)–O(7)#2	179.3(2)	O(3)#2–Cu(4)–O(8)	86.17(17)
O(6)#1–Cu(3)–O(7)#2	87.52(17)	N(1)–Cu(4)–O(8)	94.9(2)
O(9)–Cu(3)–O(7)#3	91.39(18)	O(5)#4–Cu(4)–O(4)#2	92.02(19)
N(2)–Cu(3)–O(7)#3	95.44(19)	O(3)#2–Cu(4)–O(4)#2	95.28(17)
O(6)#1–Cu(3)–O(7)#3	82.51(16)	N(1)–Cu(4)–O(4)#2	89.19(18)
O(7)#2–Cu(3)–O(7)#3	84.25(16)	O(8)–Cu(4)–O(4)#2	91.58(17)
O(9)–Cu(3)–O(8)	99.98(18)	O(7)#2–Cu(3)–O(8)	82.18(15)
N(2)–Cu(3)–O(8)	98.26(18)	O(7)#3–Cu(3)–O(8)	161.62(15)
O(6)#1–Cu(3)–O(8)	84.57(16)		

[a] Symmetry transformations used to generate equivalent atoms: #1: $-x+1, -y, -z+1$; #2: $-x, -y, -z+1$; #3: $x+1, y, z$; #4: $x, y-1, z$.

Table 3. Selected bond lengths (Å) and angles (°) for compound **2**.[a]

Mo(1)–O(8)	1.730(5)	Mo(2)–O(1)	1.728(5)
Mo(1)–O(6)#1	1.755(5)	Mo(2)–O(2)	1.730(5)
Mo(1)–O(5)	1.765(4)	Mo(2)–O(3)#2	1.772(5)
Mo(1)–O(7)	1.783(5)	Mo(2)–O(4)#3	1.798(4)
Cu(1)–O(4)	1.987(4)	Cu(2)–O(3)	1.951(5)
Cu(1)–N(3)	2.002(5)	Cu(2)–O(7)	2.002(5)
Cu(1)–N(1)	2.016(5)	Cu(2)–N(2)	2.029(6)
Cu(1)–O(5)	2.044(4)	Cu(2)–N(4)	2.024(5)
Cu(1)–O(6)	2.044(5)	Cu(2)–O(2)	2.115(5)
O(8)–Mo(1)–O(6)#1	109.3(2)	O(1)–Mo(2)–O(2)	108.3(3)
O(8)–Mo(1)–O(5)	107.8(2)	O(1)–Mo(2)–O(3)#2	106.4(2)
O(6)#1–Mo(1)–O(5)	109.7(2)	O(2)–Mo(2)–O(3)#2	110.5(2)
O(8)–Mo(1)–O(7)	110.2(3)	O(1)–Mo(2)–O(4)#3	110.3(2)
O(6)#1–Mo(1)–O(7)	110.6(2)	O(2)–Mo(2)–O(4)#3	110.4(2)
O(5)–Mo(1)–O(7)	109.1(2)	O(3)#2–Mo(2)–O(4)#3	110.8(2)
O(4)–Cu(1)–N(3)	92.0(2)	O(3)–Cu(2)–O(7)	145.4(2)
O(4)–Cu(1)–N(1)	91.3(2)	O(3)–Cu(2)–N(2)	92.1(2)
N(3)–Cu(1)–N(1)	176.7(2)	O(7)–Cu(2)–N(2)	90.5(2)
O(4)–Cu(1)–O(5)	127.2(2)	O(3)–Cu(2)–N(4)	87.5(2)
N(3)–Cu(1)–O(5)	87.9(2)	O(7)–Cu(2)–N(4)	90.3(2)
N(1)–Cu(1)–O(5)	90.1(2)	N(2)–Cu(2)–N(4)	179.2(2)
O(4)–Cu(1)–O(6)	121.1(2)	O(3)–Cu(2)–O(2)	114.7(2)
N(3)–Cu(1)–O(6)	88.8(2)	O(7)–Cu(2)–O(2)	99.9(2)
N(1)–Cu(1)–O(6)	89.5(2)	N(2)–Cu(2)–O(2)	88.5(2)
O(5)–Cu(1)–O(6)	111.7(2)	N(4)–Cu(2)–O(2)	91.0(2)

[a] Symmetry transformations used to generate equivalent atoms: #1: $-x, -y, -z$; #2: $-x+1, -y+1, -z-1$; #3: $-x+1, -y, -z$.

The structure was solved by direct methods using the program SHELXS-97 [20] and refined by full-matrix least-squares methods on F^2 using the SHELXL-97 [21] program package. All of the non-hydrogen atoms were refined anisotropically. Positions of the hydrogen atoms attached to carbon atoms were fixed at their ideal positions. Structure solution and refinement based on 3474 independent reflections gave R_1 (wR_2) = 0.0438 (0.1197). A summary of the crystallographic data and structural determination for compound **1** is provided in table 1. Selected bond lengths and angles are listed in table 2.

For **2** the data were collected on a Rigaku R-AXIS RAPID IP diffractometer at 293 K using graphite-monochromated Mo-Kα radiation ($\lambda = 0.71073$ Å) and the oscillation scans technique in the range of $1.95° < \theta < 27.48°$. Empirical absorption correction was applied. A total of 8093 (4316 unique, $R_{int} = 0.0548$) reflections were measured. The structure was solved by direct methods using SHELXS-97 [20] and refined by full-matrix least-squares methods on F^2 using SHELXL-97 [21]. All non-hydrogen atoms were refined anisotropically. Positions of hydrogen atoms attached to carbon atoms were fixed at their ideal positions. Structure solution and refinement based on 4316 independent reflections gave R_1 (wR_2) = 0.0482 (0.1379). A summary of the crystallographic data and structural determination for compound **2** is provided in table 1. Selected bond lengths and angles are listed in table 3.

CCDC-269749 and 269750 contain the supplementary crystallographic data for compounds **1** and **2**, respectively.

Supplementary data

Crystallographic data for the structures in this article have been deposited with the Cambridge Crystallographic Data Center. These data can be obtained free of charge at www.ccdc.cam.ac.uk/conts/retrieving.html (or from the Cambridge Crystallographic Data Centre, 12, Union Road, Cambridge CB2 1EZ, UK; Fax: + 44-1223/336-033; E-mail: deposit@ccdc.cam.ac.uk).

References

[1] T. Yamase. *Chem. Rev*., **98**, 307 (1998).
[2] W.G. Klemperer, C.G. Wall. *Chem. Rev*., **98**, 297 (1998).
[3] C.L. Hill, C.M. Prosser-McCartha. *Coord. Chem. Rev*., **143**, 407 (1995).
[4] Special issue on Polyoxometalates: C.L. Hill (guest ed.). *Chem. Rev*. **1** (1998) and references therein.
[5] P.J. Hagrman, D. Hagrman, J. Zubieta. *Angew. Chem. Int. Ed*., **38**, 2638 (1999).
[6] R.L. La Duca Jr, M. Desciak, M. Laskoski, R.S. Rarig Jr, J. Zubieta. *J. Chem. Soc., Dolton Trans*., 2255 (2000).
[7] D. Hagrman, P. Hagrman, J. Zubieta. *Inorg. Chim. Acta*, **300**–**302**, 212 (2000).
[8] P.J. Hagrman, R.L. La Duca Jr, H.-J. Koo, R. Rarig Jr, R.C. Haushalter, M.-H. Whangbo, J. Zubieta. *Inorg. Chem*., **39**, 4311 (2000).
[9] S.I. Stupp, P.V. Braun. *Science*, **277**, 1242 (1997).
[10] D. Hagrman, C.J. Warren, R.C. Haushalter, C. Seip, C.J. O'Connor, R.S. Rarig, K.M. Johnson, R.L. LaDuca, J. Zubieta. *Chem. Marter*., **10**, 3294 (1998).
[11] C.-Z. Lu, C.-D. Wu, S.-F. Lu, J.-C. Liu, Q.-J. Wu, H.-H. Zhuang, J.-S. Huang. *Chem. Commun*., 152 (2002).
[12] S.-I. Noro, S. Kitagawa, M. Kondo, K. Seki. *Angew. Chem. Int. Ed*., **39**, 2082 (2000).
[13] T.K. Maji, K. Uemura, H.-C. Chang, R. Matsuda, S. Kitagawa. *Angew. Chem. Int. Ed*., **43**, 3269 (2004).
[14] X.L. Wang, C. Qin, E.B. Wang, Y.G. Li, C.W. Hu, L. Xu. *Chem. Commun*., 378 (2004).
[15] J.-L. Song, H.-H. Zhao, J.-G. Mao, K.R. Dunbar. *Chem. Mater*., **16**, 1884 (2004).
[16] S. Subramanian, M.J. Zaworotko. *Angew. Chem. Int. Ed*., **34**, 2127 (1995).
[17] J. Lü, E.H. Shen, Y.G. Li, D.R. Xiao, E.B. Wang, C.W. Hu, L. Xu. *Crystal Growth & Design*, **1**, 65 (2005).
[18] S.O. Grim, L.J. Matienzo. *Inorg. Chem*., **14**, 1014 (1975).
[19] L. Beyer, T. Kirmse, J. Stach, T. Szargan, E. Hoyer. *Z. Anorg. Allg. Chem*., **476**, 7 (1981).
[20] G.M. Sheldrick. *SHELXS 97, Program for Crystal Structure Solution*, University of Göttingen (1997).
[21] G.M. Sheldrick. *SHELXL 97, Program for Crystal Structure Refinement*, University of Göttingen (1997).